

Published in final edited form as:

*Bioorg Med Chem Lett.* 2013 October 1; 23(19): . doi:10.1016/j.bmcl.2013.07.056.

## C-peptide inhibitors of Ebola virus glycoprotein-mediated cell entry: Effects of conjugation to cholesterol and side chain–side chain crosslinking

Chelsea D. Higgins<sup>a</sup>, Jayne F. Koellhoffer<sup>a</sup>, Kartik Chandran<sup>b</sup>, and Jonathan R. Lai<sup>a,\*</sup>

<sup>a</sup>Department of Biochemistry, Albert Einstein College of Medicine, Bronx, NY 10461, USA

<sup>b</sup>Department of Microbiology and Immunology, Albert Einstein College of Medicine, Bronx, NY 10461, USA

### Abstract

We previously described potent inhibition of Ebola virus entry by a ‘C-peptide’ based on the GP2 C-heptad repeat region (CHR) targeted to endosomes (‘**Tat-Ebo**’). Here, we report the synthesis and evaluation of C-peptides conjugated to cholesterol, and **Tat-Ebo** analogs containing covalent side chain–side chain crosslinks to promote  $\alpha$ -helical conformation. We found that the cholesterol-conjugated C-peptides were potent inhibitors of Ebola virus glycoprotein (GP)-mediated cell entry ( $\sim 10^3$ -fold reduction in infection at 40  $\mu$ M). However, this mechanism of inhibition is somewhat non-specific because the cholesterol-conjugated peptides also inhibited cell entry mediated by vesicular stomatitis virus glycoprotein G. One side chain–side chain crosslinked peptide had moderately higher activity than the parent compound **Tat-Ebo**. Circular dichroism revealed that the cholesterol-conjugated peptides unexpectedly formed a strong  $\alpha$ -helical conformation that was independent of concentration. Side chain–side chain crosslinking enhanced  $\alpha$ -helical stability of the **Tat-Ebo** variants, but only at neutral pH. These results provide insight into mechanisms of C-peptide inhibition of Ebola virus GP-mediated cell entry.

### Keywords

C-peptide; Peptide design; Viral membrane fusion; Ebola virus; Hemorrhagic fever

Ebolaviruses and marburgviruses (the ‘filoviruses’, members of the family *Filoviridae*) are causative agents of a severe and rapidly progressing hemorrhagic fever.<sup>1,2</sup> Although filovirus infections are rare in the United States and Europe, outbreaks have been occurring with increased frequency in endemic regions. In 2012 alone, the Centers for Disease Control (CDC) reported five filovirus outbreaks or isolated cases of infection in Africa: two caused by Sudan virus, SUDV, one by Bundibugyo virus, BDBV (both Ebola virus species) and two caused by Marburg virus, MARV.<sup>3</sup> In larger outbreaks, mortality rates range from 30% to 90%. Currently, there are no approved therapies or vaccines to treat filovirus infections in the United States. Due to their rapid proliferation and high mortality rates associated with infection, filoviruses are classified as Category A biodefense pathogens by the National Institutes of Allergy and Infectious Diseases (NIAID) and CDC.

© 2013 Elsevier Ltd. All rights reserved.

\*Corresponding author. jon.lai@einstein.yu.edu (J.R. Lai).

### Supplementary data

Supplementary data associated with this article can be found, in the online version, at <http://dx.doi.org/10.1016/j.bmcl.2013.07.056>.

Among the filoviruses, the Zaire Ebola virus species (EBOV) has been most extensively studied.<sup>2,4,5</sup> EBOV particles are enveloped, filamentous and contain a negatively stranded RNA genome. Infection requires fusion of the host and EBOV membranes for delivery of the viral genomic material. This process is thought to occur in host endosomal compartments and is mediated by the transmembrane glycoprotein subunit GP2.<sup>6,7</sup> In the prefusion state, the glycoprotein (GP) spike assembly consists of three copies each of the surface subunit (GP1) and the transmembrane subunit (GP2).<sup>2,4,5</sup> Cell attachment involves binding of cell surface host factors by GP1, followed by uptake of the EBOV particle by macropinocytosis. Once in the endosome, host proteases Cathepsin L and Cathepsin B (CatL and CatB, respectively) process GP1 to relieve constraints on GP2 and expose a receptor-binding domain (RBD). Interaction between the RBD and at least one host receptor, Niemann Pick C1 (NPC-1), is required to trigger membrane fusion.<sup>8</sup>

The subsequent events leading to membrane fusion are analogous to mechanisms proposed for HIV-1 and influenza, and are based mostly on structural information.<sup>2,4,5,9,10</sup> GP2 is thought to undergo a conformational transition that results in projection of its N-terminal fusion loop into the host endosomal membrane. This results in a transient intermediate known as the extended or prehairpin intermediate that spans the viral and host cell membranes. Two heptad repeat regions, N- and C-terminal (the NHR and CHR, respectively) next refold into a highly stable six-helix bundle.<sup>6,7</sup> This refolding event brings the host and virus membranes into proximity and thus facilitates initial fusion events. Ultimately, a fusion pore is formed through which the viral contents are delivered into the host cytosol. Three-dimensional structures of the core domain from EBOV and MARV GP2 in the 'post-fusion' conformation have been described and are highly similar.<sup>6,7,11</sup> The six-helix bundle contains a long, central NHR core (a triple-stranded coiled-coil) with the three shorter CHR segments packed in an antiparallel configuration. An intramolecular disulfide bond stabilizes a loop/helix-turn-helix motif between the NHR and CHR.

Evidence for the extended intermediate in most 'class I' fusion proteins (i.e., those that contain  $\alpha$ -helical segments) is largely indirect.<sup>9,10</sup> Two recent reports provide specific information about interbilayer spacing and glycoprotein clustering where the extended intermediate occurs.<sup>12,13</sup> However, the major evidence for this conformation arises from the fact that synthetic peptides corresponding to the CHR ('C-peptides') can block infection.<sup>9,10</sup> It is assumed that C-peptides function by binding the preformed NHR core trimer in the transiently exposed extended intermediate, thus sequestering these segments and preventing formation of the sixhelix bundle. One HIV-1 C-peptide is an approved drug (Enfurvitide/Fuzeon/T-20).

The fusion reaction for HIV-1 occurs primarily at the cell surface, but most other membrane viruses are taken up into endosomal compartments where low pH or other endosomal factors are required to trigger membrane fusion.<sup>9,10</sup> Therefore, inhibition of viral entry within endosomes requires a C-peptide that localizes to the sites of membrane fusion. We previously reported potent and broad-spectrum inhibition of filovirus infection by an EBOV C-peptide consisting of the CHR segment appended to an arginine-rich cell-penetrating undecapeptide from HIV-1 transactivator protein ('**Tat-Ebo**').<sup>12</sup> Here we explore the effect of two peptide modifications on the activity of EBOV C-peptides: conjugation to cholesterol and side chain–side chain crosslinking.

Other groups have found that HIV-1, paramyxoviruses, as well as endosomal viruses (e.g., influenza virus) can be potently inhibited by C-peptides conjugated to a cholesterol group.<sup>13–16</sup> It is believed that the cholesterol group localizes the C-peptide to membrane surfaces such that it is primed to interact with the NHR of the transient extended intermediate when it forms.<sup>13–16</sup> Presumably, this cholesterol-mediated localization effect is

not specific to endosomal or plasma membranes, explaining why both HIV-1 and influenza virus can be targeted effectively in this way. For HIV-1 C-peptides, conjugation to cholesterol confers up to 400-fold improvement in  $IC_{50}$ .<sup>13</sup> For paramyxoviruses and influenza, cholesterol conjugation imparts activity on an otherwise inactive C-peptide.<sup>14–16</sup> With these factors in mind, we designed and synthesized peptides **1** and **2** in which the EBOV GP2 CHR peptide segment contains either an N-terminal or C-terminal free cysteine as a reactive handle for conjugation. In both cases, a tetralysine segment was included to enhance solubility. Peptides **1** and **2** were produced by standard solid-phase peptide chemistry, and purified by HPLC. Cholesterol was bromoacetylated at the 3-C hydroxyl using bromoacetic acid and *N,N*-diisopropylcarbodiimide; the bromoacetylated cholesterol was conjugated to the free thiols of **1** or **2** to form **1-Chol** or **2-Chol** (Scheme 1a). We found that the cholesterol ester was stable to hydrolysis for periods of up to 72 h at neutral pH (data not shown).

The capacity for **1-Chol** or **2-Chol** to inhibit GP-mediated viral entry was assessed with a vesicular stomatitis virus particle bearing the EBOV GP in place of the native glycoprotein G ('VSV-GP').<sup>12</sup> The matrix protein contains an eGFP fusion allowing primary infection events to be quantified by fluorescence confocal microscopy. Vero cells were used as the host cell line. Peptides **1-Chol** and **2-Chol** resulted in potent inhibition of VSV-GP entry with  $\sim 10^3$ -fold reduction in infection at 40  $\mu M$  peptide concentrations (Fig. 1). This level of inhibition far exceeds previously reported VSV-GP inhibition by **Tat-Ebo**, which was  $\sim 10^2$ -fold reduction in entry at higher peptide concentrations (75  $\mu M$ ).<sup>12</sup> Notably, cholesterol alone had relatively modest effects on VSV-GP entry. However, we found that this activity was not specific to the EBOV glycoprotein. When **1-Chol** and **2-Chol** were tested for inhibition of VSV bearing its native envelope glycoprotein G ('VSV-G'), both had potent activity for inhibition of VSV-G, with  $\sim 90\%$  reduction at 10  $\mu M$  peptide concentration and  $>99\%$  reduction at higher concentrations. Importantly, both peptides exhibited only modest cell toxicity ( $\sim 20\%$ ) under these conditions (see Supplementary data). The potent inhibition of VSV-G by **1-Chol** and **2-Chol** suggests that a major aspect of the neutralization mechanism is non-specific, although the fact that cholesterol had only modest effects on VSV-GP entry suggests this mechanism requires some combination of peptide and cholesterol moieties. This behavior contrasts with that of cholesterol-conjugated C-peptides derived from other viruses.<sup>13–16</sup> For example, cholesterol-conjugated HIV-1 C-peptides had no activity against VSV-G in previous studies.<sup>13</sup> Cholesterol-conjugated C-peptides based on influenza had activity against VSV pseudotyped with influenza HA but not against VSV pseudotyped with the GPC from Nipah virus.<sup>16</sup> However, activity against the native VSV G protein was not explored in this case. Furthermore, this non-specific effect appears to be related to the cholesterol-conjugated peptide; we previously reported that **Tat-Ebo** has no activity against VSV-G at 75  $\mu M$ .<sup>12</sup>

To further explore requirements for inhibition of viral entry by cholesterol-conjugated peptides, we produced **3-Chol**, a peptide that consists of a tetralysine segment conjugated to cholesterol. We found **3-Chol** was active against both VSV-GP and VSV-G (Fig. 1). Binding to the NHR should be dependent on inclusion of the CHR sequence, which is not present in **3-Chol**. At 20  $\mu M$ , **3-Chol** is much less potent against VSV-GP than **1-Chol** and **2-Chol**, suggesting that some component of activity is dependent on the native CHR sequence. However, at higher concentrations, **3-Chol** inhibits VSV-GP entry by  $>90\%$ . These results indicate a non-specific component of VSV-GP inhibition by cholesterol-conjugated peptides since **3-Chol** does not contain the GP CHR sequence. In contrast, we previously reported that inhibition of VSV-GP entry by **Tat-Ebo** was dependent on the native GP2 CHR sequence since a sequence isomer in which the CHR segment was scrambled had no effect on entry.<sup>12</sup>

The non-specific contribution to inhibitory activity against VSV-GP is further exemplified by the fact that **1-Chol** is more potent than **2-Chol**. The orientation of the NHR core trimer  $\alpha$ -helices is thought to be directional in the extended intermediate (with the N-terminal end pointed toward the cell membrane). It was therefore predicted that **2-Chol** would be more potent than **1-Chol** because the C-terminal location of the cholesterol in **2-Chol** should affix the C-peptide in the native antiparallel orientation relative to the NHR in the extended intermediate. For HIV-1 C-peptides containing N- or C-conjugated cholesterol, the C-terminal conjugated C-peptide has >2000-fold higher activity than the N-terminal conjugated peptide.<sup>13</sup> However, **1-Chol** is more potent than **2-Chol**, indicating that the orientation of the C-terminal end of the C-peptide toward the membrane is not an important factor for potency. This result suggests either that the C-peptide is liberated from the cholesterol group during infection, or that inhibition involves a more complex mechanism.

We sought to evaluate a second strategy for improvement of antiviral properties of EBOV C-peptides by incorporation of structure-promoting modifications. The activity of the CHR segment in **Tat-Ebo** is likely dependent on  $\alpha$ -helical conformation, since the native CHR segment participates in a six-helix bundle in the post-fusion core domain structure.<sup>6,7</sup> Therefore, enforcing an  $\alpha$ -helical structure by side chain–side chain cross-links is expected to enhance activity of **Tat-Ebo**. To test this hypothesis, we produced peptides **4** and **5**, which contain Cys and Orn residues at  $i$  and  $i + 3$  positions that are not expected to impact CHR binding according to the post-fusion GP2 structure. Dawson and coworkers demonstrated that a thioetheramide side chain–side chain crosslink between Cys and Orn residues at this spacing provides proper geometry and length to promote  $\alpha$ -helical structure.<sup>17,18</sup> Peptides **4** and **5** were produced using standard N-FMOC strategy with acid labile protecting groups on all side chains except the Orn residues, which were protected with an N $\epsilon$ -ALLOC group. Treatment of the resin-bound peptide precursors with triphenylphosphine Pd(0) resulted in deprotection of the Orn side chain as determined by positive Kaiser test. The Orn free amine was iodoacetylated using iodoacetic anhydride. Treatment of this resin with TFA resulted in simultaneous cleavage and side chain deprotection. Formation of the thioether amide was rapid and spontaneous to yield **4-Link** and **5-Link**. Final products were purified by RP-HPLC, and all masses were confirmed by MALDI-MS (Table 1).

Peptide **4-Link** provided potent neutralization of VSV-GP, with ~99% reduction (2 logs) in infection at 40  $\mu$ M (Fig. 2). At this concentration, **4-Link** was well tolerated by Vero cells as scored by visual inspection of the cells (data not shown) and a commercial cell viability assay (see Supplementary data). The potency of **4-Link** is moderately higher than our previous studies on **Tat-Ebo**, which afforded 99% reduction only at concentrations of 75  $\mu$ M.<sup>12</sup> Interestingly, **4-Link** was able to inhibit infection of VSV-G as well, though to a lesser extent than VSV-GP at high concentrations. At 40  $\mu$ M, ~80% (<1 log) reduction in VSV-G infection was observed whereas 2 logs of inhibition were observed in VSV-GP. Therefore, there is some specificity for **4-Link** activity toward the EBOV GP. Vero cells incubated with concentrations of **5-Link** exceeding 15  $\mu$ M showed signs of toxicity by visual inspection (not shown), which prevented assessment of antiviral activity at higher concentrations. At lower concentrations, **5-Link** inhibited both VSV-GP and VSV-G with similar potency. It is interesting to note that that **4-Link** and **5-Link** had activity against VSV-G, since the parent compound **Tat-Ebo** was highly specific for VSV-GP over VSV-G (Ref. 12). It is possible that incorporation of side chain–side chain crosslinks results in general effects of cellular toxicity (as in the case of **5-Link**) or disruption of endosomal uptake mechanisms (**4-Link**).

We next sought to explore the structural properties of **1-Chol**, **2-Chol**, **4-Link**, and **5-Link** to determine if their propensities to adopt  $\alpha$ -helical conformation were correlated with

activity. Circular dichroism (CD) spectra indicated surprisingly that **1-Chol** and **2-Chol** adopt a strong  $\alpha$ -helical conformation at pH 4.6 and pH 7.1 (Fig. 3). In contrast, **Lys-Ebo**, whose sequence is similar to that of **1-Chol** but does not contain the cholesterol-conjugated cysteine, did not exhibit an  $\alpha$ -helical signature. This result was unexpected; the cholesterol moiety in **1-Chol** and **2-Chol** is separated from the CHR segment by a flexible tripeptide linker (~GSG~) and a tetralysine segment in both peptides. Therefore, it is unlikely that the cholesterol induces  $\alpha$ -helical conformation by direct contacts with any of the side chain residues in the CHR segment. Another possibility is that the cholesterol group induces limited aggregation of the peptide to form  $\alpha$ -helical bundles. However, we found that the CD spectrum for **1-Chol** was similar over a 4.1–23  $\mu$ M range (see Supplementary data), suggesting that any aggregation-induced structural transitions do not take place in this concentration range.

Both **4-Link** and **5-Link** had partial  $\alpha$ -helical characteristic at pH 7.1 as indicated by a negative band at ~208 nm and a shoulder at 222 nm (Fig. 3B). It is interesting to note that **5-Link** had stronger  $\alpha$ -character than did **4-Link**, indicating that placement of the side chain–side chain crosslink has structural effects. This behavior contrasts with previous results on **Tat-Ebo** indicating this peptide is unstructured in aqueous solution.<sup>12</sup> Therefore, we conclude that the thioetheramide side chain–side chain crosslink enhances  $\alpha$ -helical conformation in **4-Link** and **5-Link**. However, we found that **4-Link** and **5-Link** had diminished  $\alpha$ -helical character at pH 4.6 relative to pH 7.1.  $\alpha$ -Helical wheel analysis suggests this pH-dependent behavior may be due to side chain–side chain interactions between Arg residues of the Tat segment and acidic or His residues of the CHR segment. For example, Arg<sub>9</sub> (at a **c** position) has the capacity to form  $\alpha$ -helix stabilizing salt bridges with Glu<sub>16</sub> (another **c** position) and Asp<sub>19</sub> (an **f** position) at neutral pH. However, such interactions would be diminished under conditions where the acidic residues are protonated. Arg<sub>11</sub> (at an **e** position) may form unfavorable electrostatic interactions with His<sub>18</sub> (an **e** position) under conditions where the imidazolium group is protonated.

Here we describe the synthesis and evaluation of modified C-peptides for the inhibition of EBOV GP-mediated cell entry. Although potent, the inhibitory effect of cholesterol-conjugated C-peptides **1-Chol** and **2-Chol** had little specificity for the glycoprotein of EBOV (VSV-GP vs VSV-G) or the native CHR sequence (**1-Chol** vs **3-Chol**). It seems reasonable that some aspect of inhibition in these peptides arises from delivery of the CHR segment to the sites of membrane fusion. However, these data also suggest additional effects, related specifically to the combination of peptide and cholesterol, contribute to this activity. The fact that inhibition with both VSV-GP and VSV-G is observed indicates that this non-specific component may include mechanisms of cellular uptake or endosomal maturation. Curiously, cholesterol conjugation enhances  $\alpha$ -helical structure in a concentration-independent manner. Whether this structural effect plays a role in the broad inhibitory activity remains to be determined. These results further suggest that caution must be exercised in considering cholesterolconjugated C-peptides as a therapeutic antiviral approach.<sup>13–16,19</sup> Furthermore, we found modest enhancement in activity with the side chain–side chain crosslinked peptide **4-Link** relative to its linear analog **Tat-Ebo**. CD indicates an enhancement in  $\alpha$ -helical structure, which may play a role in this inhibitory activity. However, it is expected that **4-Link** would function at pHs of the late endosome (pH 4.5–5.5), and under these conditions structure was not promoted. These results provide novel insights into C-peptide inhibition of the filoviruses.

## Supplementary Material

Refer to Web version on PubMed Central for supplementary material.

## Acknowledgments

We thank Wei Wang and the Albert Einstein College of Medicine Chemical Biology Core Facility for assistance with synthesis of the cholesterol-conjugated peptides, and Rohit Jangra for assistance with cellular toxicity and viral entry assays. This work was funded by the NIH (AI090249 to J.R.L. and AI088027 to K.C.). J.F.K. was supported in part by Medical Scientist Training Program T32-GM007288.

## References and notes

1. Feldmann H, Geisbert TW. *Lancet*. 2011; 377:849. [PubMed: 21084112]
2. Lee JE, Saphire EO. *Future Virol*. 2009; 4:621. [PubMed: 20198110]
3. <http://www.cdc.gov/ncidod/dvrd/spb/mnpages/dispages/ebola.htm>.
4. Lee JE, Saphire EO. *Curr. Opin. Struct. Biol*. 2009; 19:408. [PubMed: 19559599]
5. Miller EH, Chandran K. *Curr. Opin. Virol*. 2012; 2:206. [PubMed: 22445965]
6. Weissenhorn W, Carfi A, Lee KH, Skehel JJ, Wiley DC. *Mol. Cell*. 1998; 2:605. [PubMed: 9844633]
7. Malashkevich VN, Schneider BJ, McNally ML, Milhollen MA, Pang JX, Kim PS. *Proc. Natl. Acad. Sci. U.S.A.* 1999; 96:2662. [PubMed: 10077567]
8. Carette JE, Raaben M, Wong AC, Herbert AS, Obernosterer G, Mulherkar N, Kuehne AI, Kranzusch PJ, Griffin AM, Ruthel G, Dal Cin P, Dye JM, Whelan SP, Chandran K, Brummelkamp TR. *Nature*. 2011; 477:340. [PubMed: 21866103]
9. Eckert DM, Kim PS. *Annu. Rev. Biochem.* 2001; 70:777. [PubMed: 11395423]
10. Harrison SC. *Nat. Struct. Mol. Biol*. 2008; 15:690. [PubMed: 18596815]
11. Koellhoffer JF, Malashkevich VN, Harrison JS, Toro R, Bhosle RC, Chandran K, Almo SC, Lai JR. *Biochemistry*. 2012; 51:7665. [PubMed: 22935026]
12. Miller EH, Harrison JS, Radoshitzky SR, Higgins CD, Chi X, Dong L, Kuhn JH, Bavari S, Lai JR, Chandran K. *J. Biol. Chem*. 2011; 286:15854. [PubMed: 21454542]
13. Ingallinella P, Bianchi E, Ladwa NA, Wang YJ, Hrin R, Veneziano M, Bonelli F, Ketas TJ, Moore JP, Miller MD, Pessi A. *Proc. Natl. Acad. Sci. U.S. A.* 2009; 106:5801. [PubMed: 19297617]
14. Porotto M, Yokoyama CC, Palermo LM, Mungall B, Aljofan M, Cortese R, Pessi A, Moscona A. *J. Virol*. 2010; 84:6760. [PubMed: 20357085]
15. Porotto M, Rockx B, Yokoyama CC, Talekar A, Devito I, Palermo LM, Liu J, Cortese R, Lu M, Feldmann H, Pessi A, Moscona A. *PLoS Pathog*. 2010; 6:e1001168. [PubMed: 21060819]
16. Lee KK, Pessi A, Gui L, Santoprete A, Talekar A, Moscona A, Porotto M. *J. Biol. Chem*. 2011; 286:42141. [PubMed: 21994935]
17. Cardoso RM, Brunel FM, Ferguson S, Zwick M, Burton DR, Dawson PE, Wilson IA. *J. Mol. Biol*. 2007; 365:1533. [PubMed: 17125793]
18. Ingale S, Gach JS, Zwick MB, Dawson PE. *J. Pept. Sci.* 2010; 16:716. [PubMed: 21104968]
19. Pessi A, Langella A, Capitò E, Ghezzi S, Vicenzi E, Poli G, Ketas T, Mathieu C, Cortese R, Horvat B, Moscona A, Porotto M. *PLoS One*. 2012; 7:e36833. [PubMed: 22666328]

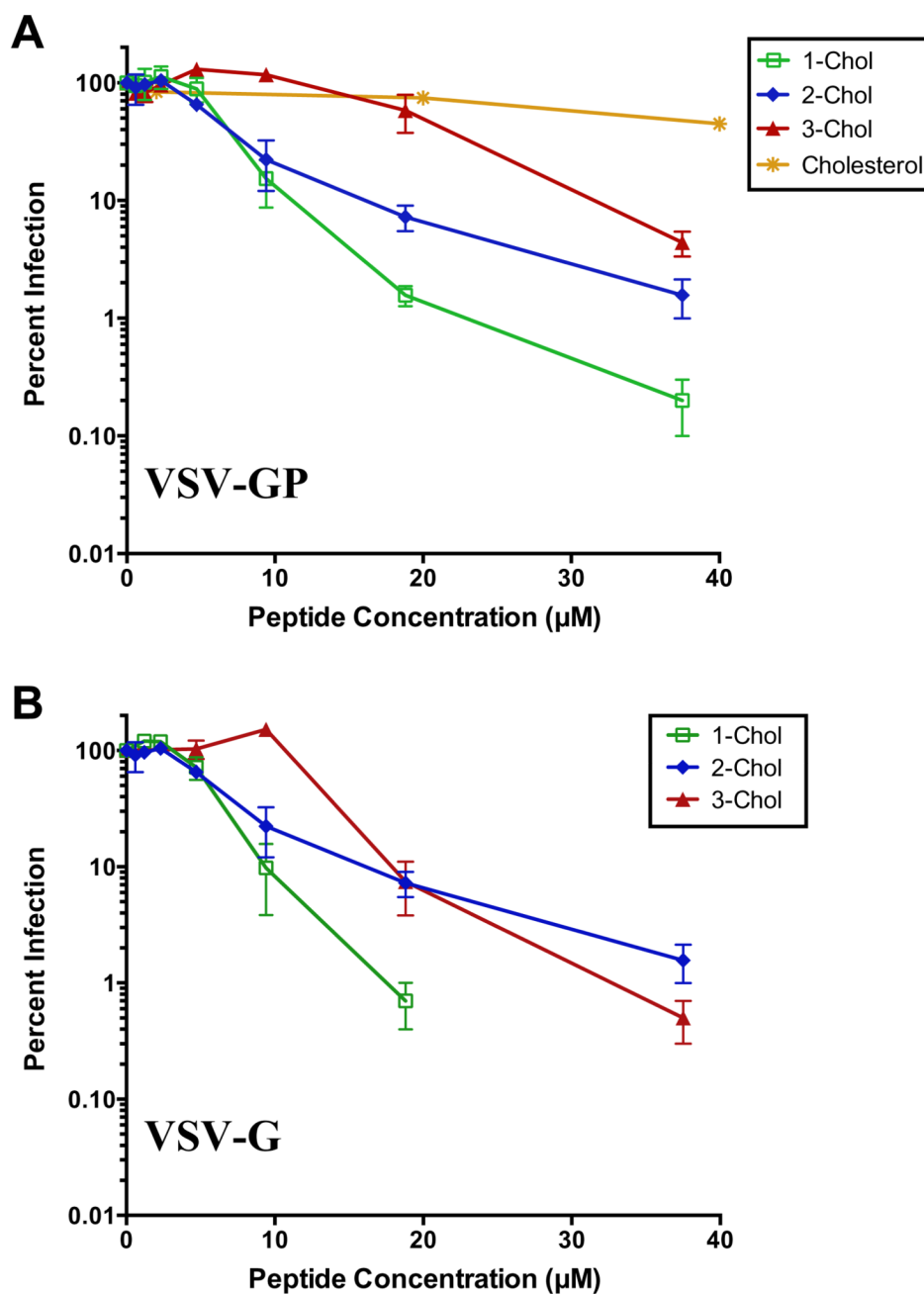
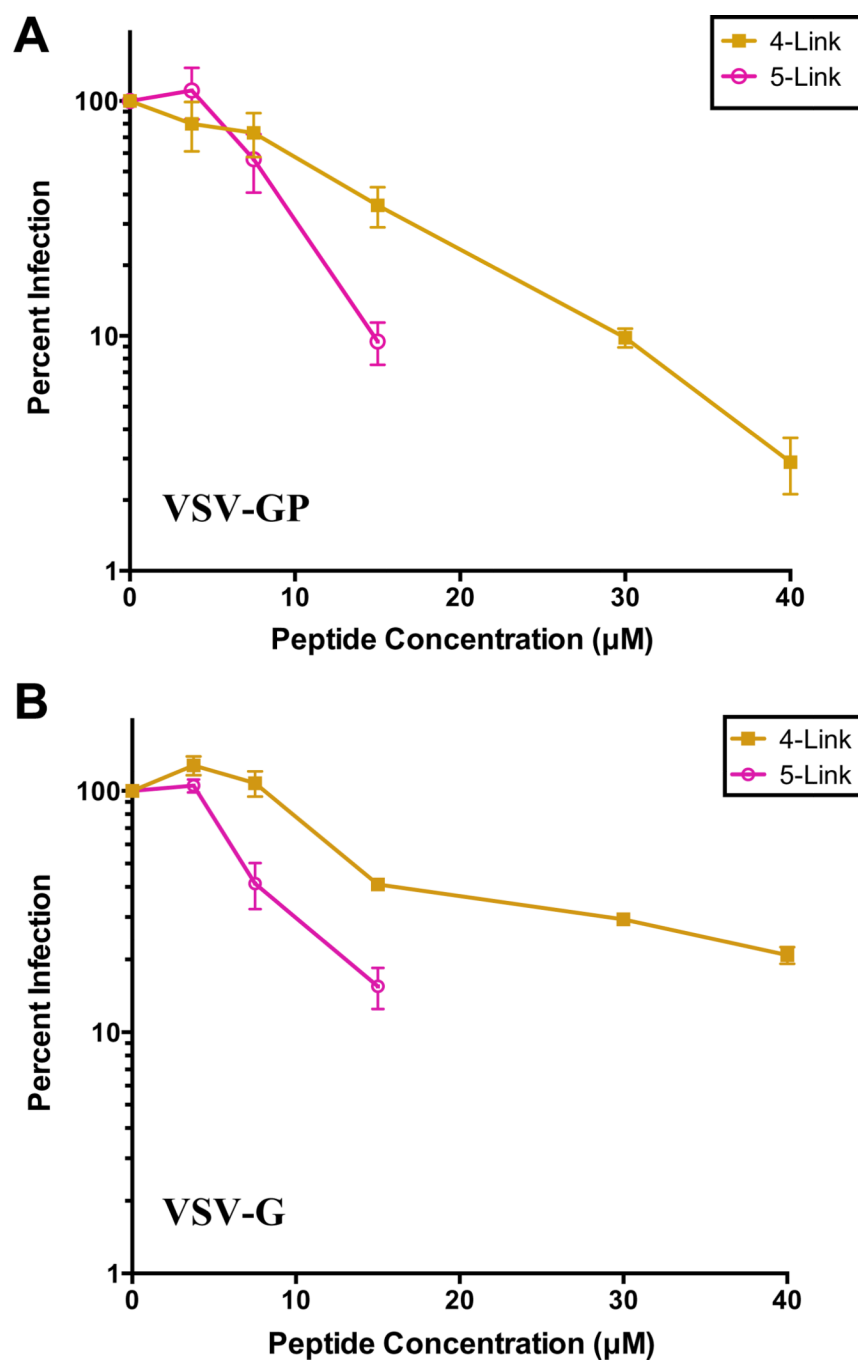


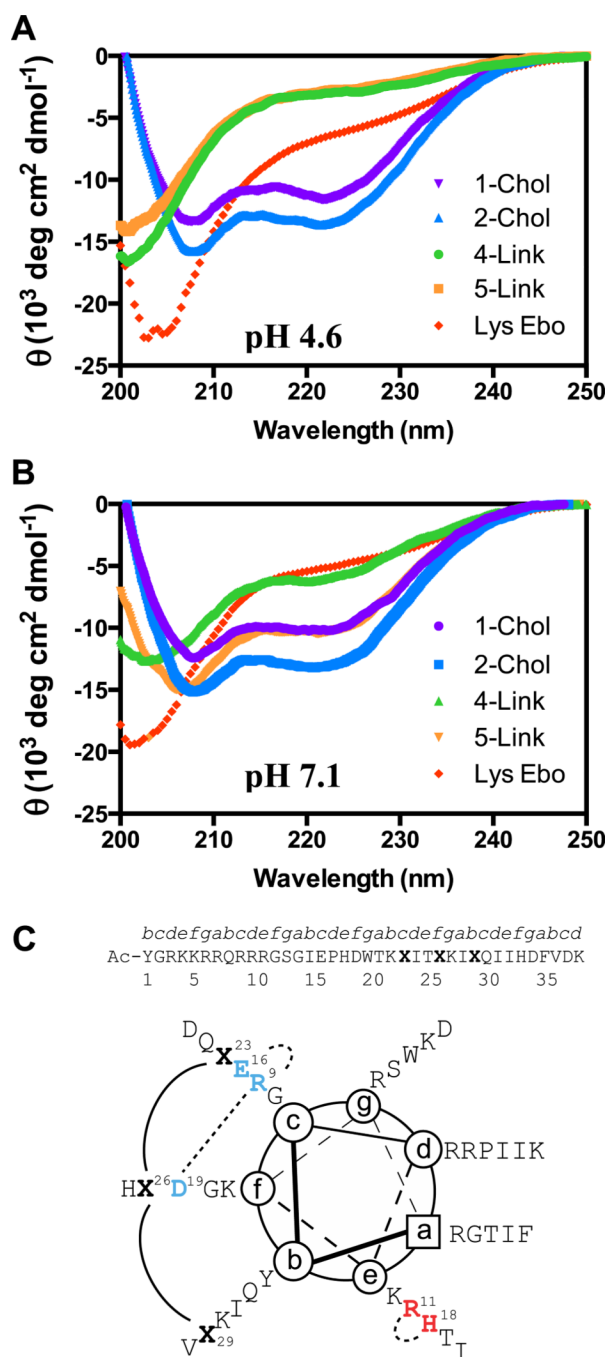
Figure 1. Inhibition of VSV-GP (A) or VSV-G (B) entry by cholesterol-conjugated peptides.

**Figure 1.**  
Inhibition of VSV-GP (A) or VSV-G (B) entry by cholesterol-conjugated peptides. For VSV-GP, cholesterol alone was included as a control.

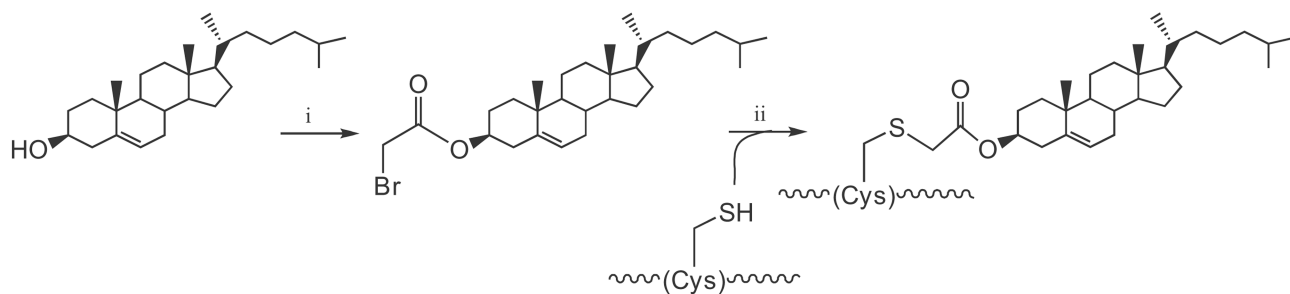
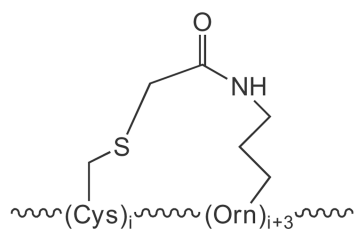


**Figure 2.** Inhibition of VSV-GP (A) or VSV-G (B) entry by side chain-side chain crosslinked peptides.





**Figure 3.** (A and B) CD spectra of peptides in 10 mM NaOAc, pH 4.6 (A), and 10 mM NaH<sub>2</sub>PO<sub>4</sub>, pH 7.1 (B). Peptide concentrations ranged from 36  $\mu$ M to 75  $\mu$ M. (C)  $\alpha$ -Helical wheel depiction of **4-Link** and **5-Link**. Potential stabilizing (blue) or destabilizing (red) interactions are shown as well as side chain–side chain crosslinks. Primary sequence and numbering shown above; ‘X’ indicates positions involved in crosslinks.

**A****B****Scheme 1.**

(A) Synthesis of cholesterol-conjugated peptides: (i) Bromoacetic acid/*N,N*-diisopropylcarbodiimide/DMAP/DCM, (ii) DMSO/DIEA; (B) Thioetheramide side chain-side chain linkage.

**Table 1**

Peptide sequences and masses

Peptide	Sequence <sup>a</sup>	[MH] <sup>+</sup> <sub>exp</sub>	[MH] <sup>+</sup> <sub>obs</sub>
<b>1</b>	CKKKKGSGIEPHDWTKNITDKIDQIIHDFVDK	3737.3	3736.8
<b>1-Chol</b>	C(Chol) <sup>b</sup> CKKKKGSGIEPHDWTKNITDKIDQIIHDFVDK	4163.9	4164.4
<b>2</b>	IEPHDWTKNITDKIDQIIHDFVDKSGGKKKCC	3737.3	3736.9
<b>2-Chol</b>	IEPHDWTKNITDKIDQIIHDFVDKSGGKKKCC(Chol) <sup>b</sup>	4163.9	4165.4
<b>3-Chol</b>	KKKKGSGC(Chol) <sup>b</sup>	1260.7	1261.0
<b>4</b>	Ac-YGRKKRRQRRRGSGIEPHDWTCKITOKIDQIIHDFVDK	4693.4	4694.5
<b>4-Link</b>	Ac-YGRKKRRQRRRGSGIEPHDWTCKITOC <sup>c</sup> KIDQIIHDFVDK	4733.4	4734.4
<b>5</b>	Ac-YGRKKRRQRRRGSGIEPHDWTCKIOQIIHDFVDK	4692.4	4694.4
<b>5-Link</b>	Ac-YGRKKRRQRRRGSGIEPHDWTCKIO <sup>c</sup> QIIHDFVDK	4732.4	4734.6
<b>Tat-Ebo</b>	YGRKKRRQRRRGSGIEPHDWTKNITDKIDQIIHDFVDK	4661.5	4661.9
<b>Lys-Ebo</b>	CKKKKGSGIEPHDWTKNITDKIDQIIHDFVDK	3633.0	3632.2

<sup>a</sup> All peptides produced as C-terminally blocked amides. In some cases, the N-terminus was blocked with an acetyl group (indicated with Ac-).

<sup>b</sup> Cholesterol conjugation to cysteine as shown in Scheme 1a.

<sup>c</sup> Thioetheramide side chain–side chain crosslink between Orn (O) and Cys as shown in Scheme 1b.